Modulation of atomic de Broglie waves using Bragg diffraction

Quantum Semiclass. Opt. **8** (1996) 497–509. Printed in the UK

Modulation of atomic de Broglie waves using Bragg diffraction

Stefan Bernet, Markus Oberthaler, Roland Abfalterer, Jörg Schmiedmayer and Anton Zeilinger

Institut für Experimentalphysik, Universität Innsbruck, Technikerstraße 25-4, A-6020 Innsbruck, Austria

Received 25 January 1996, in final form 9 February 1996

Abstract. Bragg diffraction of atoms at thick standing light waves requires that the wave-matching condition is fulfilled. This usually means that the atomic beam crosses the light wave exactly at the Bragg angle. Nevertheless, our experiments also demonstrate Bragg diffraction at detuned angles if the *amplitude* of the standing light wave is temporally modulated with an appropriate frequency. If, on the other hand, the *phase* of the light wave is modulated no diffraction is observed. Both modulation processes produce frequency sidebands which set up 'slowly travelling standing waves' in front of a retro-reflection mirror. Atoms are diffracted at these 'almost standing' light waves in a similar way to photons at the travelling sound waves in an acousto-optic modulator. The frequency of the diffracted de Broglie waves is assumed to be shifted by the intensity modulation frequency. The different results using amplitude- and phase-modulated light waves are due to interference between the diffraction contributions of the individual frequency sidebands contained in the standing light wave.

1. Introduction

Bragg diffraction of an atomic beam at standing light waves was realized for the first time by Martin *et al* [1] in 1988. Recently, the velocity and angular selectivity of Bragg scattering have been investigated experimentally by Giltner *et al* [2]. The same group realized a Mach–Zehnder-type atom interferometer with a high fringe contrast [3] using Bragg scattering at standing light waves as a highly efficient beamsplitting mechanism.

In our paper we report a diffraction experiment in the Bragg regime at a temporally modulated standing light wave, where for the first time the experimental conditions were chosen such that the modulation period was much smaller than the interaction time between the atoms and the light wave. Similar effects were also investigated in neutron diffraction experiments at vibrating mirrors [4–8]. Related experiments with atoms have been reported in [9, 10], where reflection of the atoms at a vibrating mirror, consisting of a modulated evanescent wave, was used to modulate an atomic de Broglie wave in the time domain. Another experiment employed a travelling evanescent light grating formed by two lasers with a frequency difference to produce velocity-tuned Doppleron resonances in the diffracted signal [11]. In contrast to our experiment the interaction time between atoms and light was much smaller than the modulation period. Other Doppleron experiments also employ standing waves composed of different frequencies [12–16]. There, the excitation of an atom into an excited state can be linked to the transfer of many-photon momenta by applying a correct mixture of light frequencies. Nevertheless, Doppleron transitions change the

1355-5111/96/030497+13$19.50

internal state of an atom leading typically from the ground state to an excited state. Bragg diffraction, on the other hand, does not change the internal state of the atom, which makes it easy to exclude spontaneous emission by detuning the light frequency far enough from resonance. In [12] Doppleron and Bragg diffraction are distinguished clearly, and a hybrid multiphoton process which is closely related to our experiment is described theoretically. Our experiment is also related to quantum localization experiments by Moore *et al* [17], where atoms caught in a magneto-optical trap interact with amplitude- or phase-modulated standing light waves in order to transfer multiple resonant kicks to the atoms.

In the following, we will give a short introduction to the differences between matter–wave diffraction at thin and thick light gratings, and then discuss Bragg scattering at temporally modulated light fields.

2. Diffraction regimes

Elastic matter–wave scattering at light waves can be separated into two main regimes distinguished by the length Δz of the atom–light interaction region.

Raman–Nath and Bragg diffraction correspond to the diffraction at thin and thick standing light waves, respectively. In both cases the wave-matching condition $\vec{k}'_{\mathrm{A}} = \vec{k}_{\mathrm{A}} \pm n\vec{k}_{\mathrm{G}}$ with the requirement $|\vec{k}'_{\mathrm{A}}| = |\vec{k}_{\mathrm{A}}|$ is fulfilled, corresponding to energy and momentum conservation. Here, $\vec{k}_{\mathrm{A}}$ and $\vec{k}'_{\mathrm{A}}$ are the wavevectors of the original and the diffracted atomic de Broglie waves, $\vec{k}_{\mathrm{G}}$ is the grating vector of the light intensity grating, and n is an integer which corresponds to the diffraction order. In the case of a standing wave formed by two exactly counterpropagating light waves with wavevectors $\pm\vec{k}_{\mathrm{L}}$, the grating vector can be expressed as $\vec{k}_{\mathrm{G}} = 2\vec{k}_{\mathrm{L}}$. In this case, the wave-matching condition can be fulfilled only at special angles of incidence θ_n given by the Bragg equation:

$$\sin\theta_n = nk_{\mathrm{L}}/k_{\mathrm{A}}\,. \tag{1}$$

Atoms incident at other angles just pass the light wave without being diffracted.

The difference between Raman–Nath and Bragg diffraction regimes can be attributed to a different angular distribution of the light wavevectors $\vec{k}_{\mathrm{L}}$. By confining the light to the finite size of the interaction region Δz, an angular uncertainty for the photon momentum of $\Delta\Phi = \Delta k_{\mathrm{L}}/k_{\mathrm{L}} \geqslant 1/(2\Delta z k_{\mathrm{L}})$ results [12] due to the uncertainty principle $\Delta z\hbar\Delta k_{\mathrm{L}} \geqslant \hbar/2$. Therefore the wave-matching condition can be fulfilled in the angular range $\Delta\Phi$ around the central Bragg angle. If $\Delta\Phi$ is larger than the diffraction angle, then the angular selectivity is lost, corresponding to the case of Raman–Nath diffraction. The inverse case is obtained if

$$\Delta z > \frac{k_{\mathrm{A}}}{2nk_{\mathrm{L}}^2} \tag{2}$$

and corresponds to the Bragg diffraction regime.

An additional condition for sharply defined Bragg diffraction is that the interaction strength between the light grating and the atoms has to be small enough that no significant scattered wave amplitude arises before travelling at least a distance Δz given by equation (2) in the light crystal. Practically, this condition requires that the potential seen by the atoms ($\sim\hbar\omega_{\mathrm{Rabi}}$, where ω_{Rabi} is the intensity and frequency-detuning dependent Rabi frequency of the electronic transition [18]) is much lower than the photon recoil energy $\hbar^2k_{\mathrm{L}}^2/(2m)$. Thus, the additional condition for Bragg scattering is

$$\hbar^2k_{\mathrm{L}}^2/(2m) \gg \hbar\omega_{\mathrm{Rabi}}\,. \tag{3}$$

The inverse case would give rise to several diffracted beams simultaneously and to a loss of the angular selectivity [19, 20]. A detailed comparison of the diffraction regimes is given in [21].

3. Photon versus matter–wave Bragg diffraction

A different point of view based on real space instead of momentum space is usually applied in conventional optics, for Bragg diffraction of photons at thick gratings, holograms or crystals. Here, the critical parameter is the number of grating planes, which are crossed by any of the diffracted or undiffracted beams on their paths through the crystal. If less than one grating plane is crossed, the grating can be treated as two-dimensional. The far-field diffraction properties of such a thin grating are determined by Fourier transforming the transfer function of the grating, which is thus treated as a spatial amplitude and phase filter [22]. This cannot work if more than one grating plane is crossed, because a simple spatial filter would lose its position-dependent variation due to averaging. Instead, in this case a diffracted wave inside the crystal has to be taken into consideration from the beginning, resulting in a coupling of diffracted and undiffracted waves. Such a picture is applied in dynamical diffraction theories for matter and light waves [18, 19, 23].

The situation is sketched in figure 1. A standing light intensity grating with a period of $d_G = 2\pi/k_G$ is formed by retro-reflection of a plane light wave with a wavevector $k_L = k_G/2$ at an adjustable mirror (the lines parallel to the mirror surface indicate the intensity maxima of the standing light wave). In first order the grating constant is independent from a small tilt angle of the mirror with respect to the perpendicular direction. The grating planes are always parallel to the mirror surface. Therefore, a change of the mirror angle translates into an equal change of the angle between the atomic beam and the light grating. If this angle corresponds to the Bragg angle θ_B then the atomic beam is coherently split and diffracted

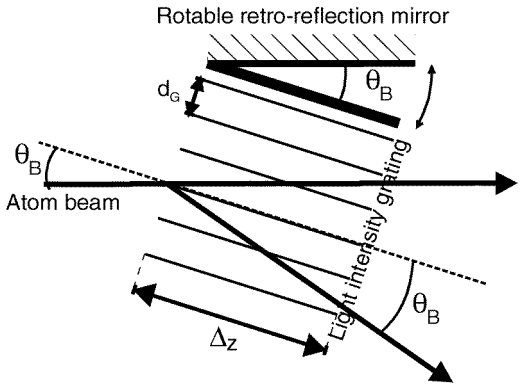

Figure 1. Geometry of a Bragg diffraction experiment, where the angle between the incident atomic beam and the standing light wave can be varied at an adjustable mirror. The standing wave is set up by retro-reflection of a plane light wave incident almost perpendicular to the mirror and to the atomic beam direction. Planes of constant light intensity within the standing intensity grating are indicated by the thin lines. They are always parallel to the mirror surface. The grating constant of the standing wave is $d_G = \lambda_L/2$ where λ_L is the light wavelength. The length, Δz, of the light crystal corresponds to the spot size of the plane light wave on the retro-reflection mirror. If the mirror angle corresponds to the Bragg angle θ_B, then diffraction into one diffraction order is observed. The number, N, of grating planes which are traversed by both the diffracted and the undiffracted parts of the atomic beam are equal: $N = \Delta z \tan\theta_B/d_G$.

into a direction corresponding to a direct reflection at the mirror surface. From figure 1 it is obvious that the number of grating planes N crossed by a wave incident at the nth-order Bragg angle θ_n is

$$N = \frac{\Delta z}{d_G} \tan\theta_n \approx \frac{\Delta z n k_L}{d_G k_A} = \frac{n k_L^2 \Delta z}{\pi k_A} . \tag{4}$$

The approximation is valid with an accuracy of 4% for Bragg angles $\theta_n < 20^\circ$. Thin (Raman–Nath) and thick (Bragg) diffraction regimes are identified by the conditions $N < 1$ or $N > 1$, respectively. The interaction length corresponding to the borderline $N = 1$ between Bragg and Raman–Nath diffraction is $\Delta z = \pi k_A/(n k_L^2)$. Compared to the result obtained above (equation (2)), the functional dependences agree within a factor of 2π.

Practically, the distinction between thin and thick gratings results in qualitatively different diffraction properties. In the (thin) Raman–Nath regime diffraction of an incoming plane wave occurs within a broad range of incidence angles and wavelengths. Furthermore, diffraction is symmetrical into conjugated orders. Therefore, even in the case of non-absorbing gratings, the maximal diffraction efficiency which is the intensity in one diffraction order normalized by the incoming intensity is limited to 33.9% [22]. On the other hand, in the Bragg case the diffraction is angle and wavelength selective. Diffraction happens only if the incidence angle is matched to the frequency, otherwise the incoming wave passes the crystal without being diffracted. In the coupled-wave theory for Bragg diffraction at material gratings, it is shown that the relative angle and wavelength (velocity) selectivity corresponds to the inverse number of grating planes which are crossed by a beam incident with the Bragg angle on a straight trajectory through the crystal [23]:

$$\frac{\Delta\theta}{\theta} = \frac{\Delta k_A}{k_A} = \frac{1}{N} = \frac{\pi k_A}{n k_L^2 \Delta z} . \tag{5}$$

The reciprocal dependence of the velocity (wavevector) selectivity on the diffraction order has been demonstrated experimentally for atomic de Broglie wave diffraction by Giltner *et al* [2].

An additional feature of the Bragg regime is that, at a given angle of incidence, at most one diffracted beam appears. Thus, in the case of non-absorbing refractive index gratings, a diffraction efficiency of 100% can be reached. Furthermore, the intensity oscillates between the diffracted and undiffracted beam as a function of the crystal length or the potential modulation index—the so-called 'pendellösung' phenomenon.

4. Bragg diffraction at travelling waves

It should be noted first that in the following we will interpret our investigated Bragg diffraction behaviour at temporally modulated light crystals as diffraction at travelling light waves, which do not actually exist. If all frequency sidebands of the complete temporally modulated light field are considered, then the result is simply a spatially stationary and temporally modulated light crystal. Nevertheless, in our observed Bragg diffraction processes only two frequency components of the light field were involved at a time. By considering only these two components, a travelling 'sub'-grating can be constructed whose diffraction properties are easily obtained. This is not the direct way of describing such an interaction, but it might give a more intuitive insight into the observed phenomena than a direct approach by solving a time-dependent Schrödinger equation.

The example of an acousto-optic modulator shows that Bragg diffraction of photons can be obtained at travelling material gratings. This is the analogue to the case of matter-waves

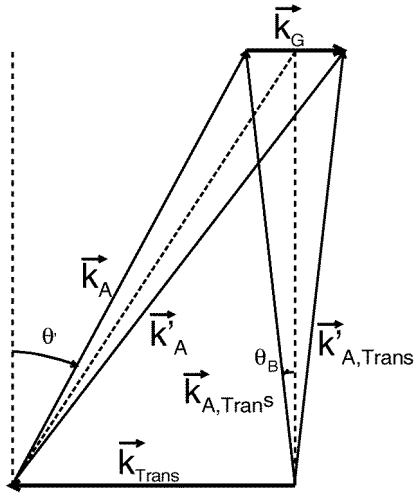

Figure 2. Illustration of the wave-matching condition for diffraction at a travelling wave. The wavevectors which are involved are: $\vec{k}_A$ and $\vec{k}'_A$, which are the wavevectors of the incoming and diffracted atomic beams in the laboratory system, respectively; $\vec{k}_{A,Trans}$ and $\vec{k}'_{A,Trans}$, which are the same wavevectors in a reference frame moving with velocity $\vec{v}_M$ parallel to the grating vector $\vec{k}_G$ of the light intensity grating, and $\vec{k}_{Trans} = -m\vec{v}_M/\hbar$ which has to be added to the atomic wavevectors in the laboratory system in order to perform the coordinate transformation. It is important to note that the light grating vector $\vec{k}_G$ is identical in both coordinate systems. The illustration shows that a direct transition $\vec{k}'_A = \vec{k}_A + \vec{k}_G$ is not possible, because the wave-matching condition requires a symmetrical triangle $\vec{k}_A$, $\vec{k}'_A$ and $\vec{k}_G$. Nevertheless, the wave-matching condition is fulfilled in a reference frame of a light wave moving with velocity $\vec{v}_M$, because of the different transformations of the atomic and the light wavevectors. The result is the same as in the direct transition: $\vec{k}'_A = \vec{k}_A + \vec{k}_G$, but diffraction is only obtained if the light intensity grating propagates with the particular velocity $\vec{v}_M$.

diffracted at propagating light gratings. For the production of a moving light intensity grating, it is sufficient to superpose two counterpropagating light waves with a frequency difference ω_M. The resulting intensity grating travels in the direction of the higher frequency wave with a velocity v_M:

$$v_M = \frac{\omega_M \lambda_L}{4\pi} = \frac{\omega_M}{2k_L} \,. \tag{6}$$

For diffraction at such a light wave the Bragg angle has to be matched to the travelling wave velocity. The reason is that a coordinate transformation into the inertial frame of the travelling wave results in a different angle between the atomic beam and (now) standing light wave. This is due to the fact that the transformation yields a significant change of the atomic wavevector component in the propagation direction of the intensity grating, whereas the light grating vector remains constant. Figure 2 shows the situation. The incoming atomic wavevector $\vec{k}_A$ cannot be diffracted by the direct process $\vec{k}'_A = \vec{k}_A + \vec{k}_G$, at a stationary light grating with wavevector $\vec{k}_G$ into the $\vec{k}'_A$ state, because the wave-matching condition is not fulfilled. The length and hence the energy of the diffracted de Broglie wave would change. Nevertheless, this diffraction process is enabled by the less apparent means of diffraction at a travelling grating. If the light intensity grating propagates with the velocity $\vec{v}_M$ parallel to its grating vector, then a coordinate transform into its frame of rest adds a vector $\vec{k}_{Trans} = -m\vec{v}_M/\hbar$ to the incoming atomic wavevector $\vec{k}_{A,Trans} = \vec{k}_A + \vec{k}_{Trans}$, whereas

the light grating vector remains constant. At two specific velocities, $\vec{v}_{\mathrm{M}}$, the wave-matching condition is fulfilled and the de Broglie wave is diffracted, which means that the grating vector $\vec{k}_{\mathrm{G}}$ adds to the atomic wavevector: $\vec{k}'_{\mathrm{A,Trans}} = \vec{k}_{\mathrm{A,Trans}} + \vec{k}_{\mathrm{G}}$. In figure 2 only one of the possibilities is drawn, for reasons of clarity, where the atomic wavevector is diffracted into one of the two Bragg orders. The other possibility corresponds to diffraction into the conjugated order and is obtained by inverting the sign of $\vec{k}_{\mathrm{G}}$ (actually a grating must always be represented by two grating vectors in opposite directions). Transforming the result back into the laboratory frame by subtracting $\vec{k}_{\mathrm{Trans}}$ yields the diffracted wavevector $\vec{k}'_{\mathrm{A}} = \vec{k}_{\mathrm{A}} + \vec{k}_{\mathrm{G}}$. Thus, momentum conservation is fulfilled as in the case of diffraction at a stationary wave, but the length of the diffracted wavevector has changed by $\Delta k'_{\mathrm{A}} = k_{\mathrm{Trans}} k_{\mathrm{G}} / k_{\mathrm{A}}$. The corresponding change of the atom's kinetic energy $\Delta E = \hbar^2 k_{\mathrm{A}} \Delta k_{\mathrm{A}} / m = \hbar \omega_{\mathrm{M}}$ is transferred by the two different photon frequencies of the absorption and stimulated emission processes. The geometry of figure 2 shows that the new angle of incidence, θ', where diffraction at the travelling wave occurs, differs from the stationary Bragg angle θ_{B} by

$$\Delta\theta = \theta' - \theta_{\mathrm{B}} \approx \frac{k_{\mathrm{Trans}}}{\sqrt{k_{\mathrm{A}}^2 - (k_{\mathrm{G}}/2)^2}} \approx \frac{\omega_{\mathrm{M}}}{k_{\mathrm{G}} v_{\mathrm{A}}} \,. \tag{7}$$

The approximations are valid to first order in k_{Trans} corresponding to the case where the atomic beam velocity, v_{A}, is much larger than the velocity of the travelling light intensity grating, v_{M}, which is always fulfilled in our experiment. If required, an exact solution can be obtained by analytically solving the geometric problem depicted in figure 2. If the Bragg angle is altered by tilting the standing light wave by $\Delta\theta$, then the direction of the atomic beam diffracted at the propagating light crystal changes only by a small amount $\Delta\phi$ from the stationary case:

$$\Delta\phi \approx \frac{1}{2}\left(\frac{k_{\mathrm{G}}}{k_{\mathrm{A}}}\right)^2 \Delta\theta \,. \tag{8}$$

Due to the small grating vector as compared to the atomic wavevector, the atomic beam is diffracted almost to the same spatial position as in the unmodulated case. The modulation frequency determines only whether diffraction occurs at all, but it does not change the diffraction angle by a considerable amount. In analogy to photon diffraction by an acousto-optic modulator, the modulation frequency adds to the frequency of the diffracted atomic de Broglie wave. The sign of the frequency shift depends on the diffraction direction with respect to the propagation direction of the light wave.

5. Travelling waves by retro-reflection of modulated light waves

Our slowly travelling light wave is created by retro-reflection of an intensity- or frequency-modulated light wave at a plane mirror. In the ideal case the modulation produces two additional frequency sidebands, separated symmetrically from the centre frequency by the modulation frequency ω_{M}.

The electric field amplitude E of a modulated light wave with centre frequency ω_{L} and modulation frequency ω_{M} can be expressed as

$$E = \exp[\mathrm{i}\omega_{\mathrm{L}} t + \mathrm{i}(\eta_0 + \eta_1 \sin\omega_{\mathrm{M}} t)] \,. \tag{9}$$

Here, the complex modulation index is considered to be composed of a constant term η_0 and a time-dependent harmonic perturbation $\eta_1 \sin\omega_{\mathrm{M}} t$. The effects of phase modulation and of amplitude modulation can be calculated simultaneously for the same modulation frequency, by composing the complex modulation index using both a real phase modulation

term β and a real amplitude modulation term α according to $\eta_0 = \beta_0 + \mathrm{i}\alpha_0$ and $\eta_1 = \beta_1 + \mathrm{i}\alpha_1$. Note, that the term α_0 yields half of the mean intensity absorption coefficient of the modulation (according to $I/I_0 = |E|^2/|E_0|^2 \sim \mathrm{e}^{-2\alpha_0}$), whereas β_0 corresponds to a constant phase offset. For a modulation without gain, the restriction $\alpha_1 < \alpha_0$ has to be fulfilled.

For a small modulation amplitude, η_1, the electric field of the modulated wave can be expanded into first-order Taylor terms:

$$E = \exp[\mathrm{i}\eta_0]\{\exp[\mathrm{i}\omega_\mathrm{L} t] + \tfrac{1}{2}\eta_1 \exp[\mathrm{i}(\omega_\mathrm{L} + \omega_\mathrm{M})t] - \tfrac{1}{2}\eta_1 \exp[\mathrm{i}(\omega_\mathrm{L} - \omega_\mathrm{M})t]\} . \tag{10}$$

The constant factor $\exp[\mathrm{i}\eta_0]$ in front of the bracket may be omitted. The exact solution for a high modulation index and higher-order harmonics can be calculated by expanding equation (9) into the Bessel functions of corresponding order. The three terms in the brackets correspond to the undisturbed part of the transmitted wave and to the frequency-shifted sidebands ($\pm\omega_\mathrm{M}$), respectively.

After retro-reflection of the three frequency components at the plane mirror, a superposition of different kinds of 'almost standing' waves results:

(i) Each of the three frequency components can superpose with its retro-reflected counterpart, leading to three standing waves with the same spatial phases at a sufficiently small distance from the mirror surface.

(ii) Additionally, each frequency component can superpose with its retro-reflected directly adjacent frequency. The four possible combinations correspond to four slowly propagating waves with the same absolute values of their travelling velocities:

$$v_\mathrm{M} = \pm\frac{c}{2}\frac{\omega_\mathrm{M}}{\omega_\mathrm{L}} . \tag{11}$$

Two of these four waves move towards the mirror surface, the others travel in the opposite direction.

(iii) Only the two sidebands superpose, leading to two slowly travelling waves. They move in opposite directions with the velocities $\pm 2v_\mathrm{M}$.

The decomposition of our light intensity grating into components of a certain travelling velocity is justified by the linearity of the diffraction process, and by the angular selectivity of Bragg deflection. Thus, the light wave field may be arranged such that the Bragg condition is fulfilled for one of its standing or slowly travelling waves only. Then the diffraction process selects only this light field component out of the superposition, and ignores the other contributions which do not satisfy the phase-matching condition. The resulting physical situation is almost the same as if only one single travelling wave existed.

In case (i) the superposition of the three standing waves with equal phases and almost equal wavevectors yields, at a sufficiently small distance from the mirror surface, a total resulting standing wave. This causes normal Bragg diffraction with the same phase-matching condition and therefore at the same Bragg angle as in the static case.

In case (iii), one travelling wave in each direction exists, which causes diffraction at the new Bragg angles $\theta' = \theta \pm \omega_\mathrm{M}/(k_\mathrm{L} v_\mathrm{A})$. Nevertheless, the diffraction efficiency is much lower than in cases (i) and (ii), due to the smaller light intensity caused by only one possible wave combination.

The most interesting case is (ii), where two waves travelling with the same velocity in the same direction contribute to one diffraction process. In the following, the diffraction properties at these two simultaneously travelling waves will be calculated. By completing equation (10) with its spatial part $\exp[\pm\mathrm{i}k_\mathrm{L} x]$, the propagation direction of the light waves can be expressed. For example, the two intensity gratings moving slowly away from the

mirror surface are composed of:

(i) $E_1 = \exp[\mathrm{i}\omega_\mathrm{L} t - \mathrm{i}k_\mathrm{L} x] + \frac{1}{2}\eta_1 \exp[\mathrm{i}(\omega_\mathrm{L} + \omega_\mathrm{M})t + \mathrm{i}k_\mathrm{L} x]$

(ii) $E_2 = -\frac{1}{2}\eta_1 \exp[\mathrm{i}(\omega_\mathrm{L} - \omega_\mathrm{M})t - \mathrm{i}k_\mathrm{L} x] + \exp[\mathrm{i}\omega_\mathrm{L} t + ik_\mathrm{L} x]\,.$

Constant phase factors introduced by the phase jump at the mirror surface have been omitted. The two waves E_3 and E_4 travelling in the opposite direction can be derived by inverting the sign of k_L. As an example, E_1 is composed of $\exp[\mathrm{i}\omega_\mathrm{L} t - \mathrm{i}k_\mathrm{L} x]$ corresponding to a wave with the centre frequency ω_L travelling towards the mirror surface, and $(\eta_1/2)\exp[\mathrm{i}(\omega_\mathrm{L} + \omega_\mathrm{M})t + \mathrm{i}k_\mathrm{L} x]$, corresponding to a wave with the higher frequency $\omega_\mathrm{L} + \omega_\mathrm{M}$ travelling in the opposite direction. The superposition leads to an 'almost-standing wave' travelling in a direction normal to the mirror surface with the small velocity $v_\mathrm{M} = c\omega_\mathrm{M}/(2\omega_\mathrm{L})$.

For further calculations, it is preferable to change into the reference frame of the slowly propagating waves with their travelling velocity of $v_\mathrm{M} = c\omega_\mathrm{M}/(2\omega_\mathrm{L})$. A non-relativistic coordinate transformation yields a Doppler shift $\omega_\mathrm{D} = \omega_\mathrm{M}/2$ which has to be added (subtracted) to wave components with a negative (positive) sign of k_L. In this frame, the two originally 'slowly travelling waves' E_1 and E_2 are now at rest:

$$E_1' = \exp\big[\mathrm{i}\big(\omega_\mathrm{L} + \tfrac{1}{2}\omega_\mathrm{M}\big)t - \mathrm{i}k_\mathrm{L} x\big] + \tfrac{1}{2}\eta_1 \exp\big[\mathrm{i}\big(\omega_\mathrm{L} + \tfrac{1}{2}\omega_\mathrm{M}\big)t + \mathrm{i}k_\mathrm{L} x\big]$$
$$E_2' = -\tfrac{1}{2}\eta_1 \exp\big[\mathrm{i}\big(\omega_\mathrm{L} - \tfrac{1}{2}\omega_\mathrm{M}\big)t - \mathrm{i}k_\mathrm{L} x\big] + \exp\big[\mathrm{i}\big(\omega_\mathrm{L} - \tfrac{1}{2}\omega_\mathrm{M}\big)t + \mathrm{i}k_\mathrm{L} x\big]\,.$$

The total electric field component E_T', of the two waves is obtained by adding both contributions, which yields:

$$\begin{aligned} E_\mathrm{T}' &= \exp[\mathrm{i}\omega_\mathrm{L} t]\big\{\exp\big[-\tfrac{1}{2}\mathrm{i}\omega_\mathrm{M} t + \mathrm{i}k_\mathrm{L} x\big] + \exp\big[\tfrac{1}{2}\mathrm{i}\omega_\mathrm{M} t - \mathrm{i}k_\mathrm{L} x\big] - \tfrac{1}{2}\eta_1 \exp\big[-\tfrac{1}{2}\mathrm{i}\omega_\mathrm{M} t - \mathrm{i}k_\mathrm{L} x\big] \\ &\quad + \tfrac{1}{2}\eta_1 \exp\big[\tfrac{1}{2}\mathrm{i}\omega_\mathrm{M} t + \mathrm{i}k_\mathrm{L} x\big]\big\} \\ &= \exp[\mathrm{i}\omega_\mathrm{L} t]\big\{2\cos\big(\tfrac{1}{2}\omega_\mathrm{M} t - k_\mathrm{L} x\big) + \mathrm{i}\eta_1 \sin\big(\tfrac{1}{2}\omega_\mathrm{M} t + k_\mathrm{L} x\big)\big\}\,. \end{aligned} \tag{12}$$

The two terms inside the bracket correspond to two waves travelling in opposite directions with the same velocity v_M.

In the case of an intensity modulation, the factor $\mathrm{i}\eta_1 = \mathrm{i}\beta_1 - \alpha_1$ in front of the sine function is real ($\beta_1 = 0$, $\alpha_1 \neq 0$). Therefore, the two waves can superpose to a standing wave, which is spatially stationary. Its intensity varies with the beating period $\tau_\mathrm{I} = 2\pi/\omega_\mathrm{M}$. Because this corresponds to a 'normal' standing wave in the reference frame of the travelling wave, diffraction is possible at the modified Bragg angles

$$\theta' = \theta_\mathrm{B} \pm \frac{\omega_\mathrm{M}}{2k_\mathrm{L} v_\mathrm{A}}\,. \tag{13}$$

On the other hand, in the case of a phase modulation, the factor $\mathrm{i}\eta_1 = \mathrm{i}\beta_1 - \alpha_1$ is imaginary ($\beta_1 \neq 0$, $\alpha_1 = 0$). Then a spatially stationary phase of the intensity grating exists for only half of the period $\tau_\mathrm{P} = \pi/\omega_\mathrm{M}$, followed by a phase jump of π. Diffraction at such a non-stationary grating occurs only if the transit time of the atoms is smaller than this period. If not, destructive interference between the diffraction contributions of the π-shifted intensity gratings suppresses diffraction. The small interaction time $\tau = \Delta z/v_\mathrm{A} < \pi/\omega_\mathrm{M}$ reduces the angular selectivity of the Bragg diffraction. In this case the angular uncertainty of the diffraction process ($\Delta\theta = \pi/(k_\mathrm{L}\Delta z) > \omega_\mathrm{M}/(k_\mathrm{L} v_\mathrm{A})$, obtained by inserting $\theta = k_\mathrm{L}/k_\mathrm{A}$ into equation (5)) is twice as large as the corresponding change of the Bragg angle ($\pm\omega_\mathrm{M}/(2k_\mathrm{L} v_\mathrm{A})$) due to the phase modulation. Therefore, diffraction at such a thin phase-modulated light wave cannot change the Bragg angle by a detectable amount. Another argument as to why sideband production by phase modulation should not have any effect on the atomic diffraction is that the total light field in front of the retro-reflection mirror

does not change any properties which can be 'seen' by the atoms—at least when the light frequency is detuned far enough off resonance of the atomic transition. Particularly, the spatial position of the light crystal remains constant, and no intensity fluctuations on the timescale of the modulation frequency appear, as in the case of amplitude modulation.

To summarize, only intensity-modulated light waves lead to Bragg diffraction of the atomic de Broglie waves at detuned Bragg angles. Only in this case is a spatially stationary standing wave obtained which diffracts atoms. In the case of phase modulation, the contributions of the two travelling waves yield a non-stationary light field even in the reference frame of the moving gratings, and no atomic diffraction results.

It must be mentioned that this analysis is only valid in the geometry of our experiment, where the travelling waves are created by retro-reflection of modulated light waves. If, on the other hand, the phase modulation were produced in only one of the beams, for example, by vibrating the retro-reflection mirror, diffraction would result at the detuned Bragg angles $\theta' = \theta_B \pm \omega_M/(2k_L v_A)$.

6. Experiment

In the experiment, we use a beam of metastable argon atoms. In the source the atoms are excited by a DC gas discharge to their metastable $1S_5$ state, which can be detected by our channeltron detector. The atom source is cooled with liquid nitrogen, following a design proposed by Kawanaka *et al* [24]. The thermal velocity of the cooled Ar beam has an average value of 440 m s^{-1} with a spread of approximately 60% (FWHM). After the source, the atomic beam is collimated by two slits with a width of 10 μm, separated by a distance of 1 m. The resulting divergence is less than one photon recoil ($0.35\hbar k$). The atomic beam is oriented parallel to the surface of a 6 cm long mirror, where the standing light wave is formed by retro-reflection of a 811 nm light wave with an intensity of 450 μW cm^{-2}. The angle of the mirror surface with respect to the atomic beam direction corresponds to the angle of incidence of the atomic beam into the light crystal. This mirror angle can be adjusted with a piezo-transducer with μrad precision. The absolute angle has been calibrated with an interferometric measurement as a function of the applied voltage with an accuracy of 8%. The Bragg angle of the argon beam is 28 μrad, corresponding to four grating planes which are crossed by the diffracted and the undiffracted beams on their paths through the 6 cm long light crystal. This means, that the experiments are performed in the regime of Bragg diffraction, according to equation (2), and the angular selectivity (and velocity selectivity) of the diffraction should be $\approx$25% of their mean values.

In order to form a non-absorbing refractive index grating the light produced by a stabilized diode laser with a linewidth of 1 MHz is detuned by 80 MHz from the 811 nm closed transition of the metastable argon atoms. The *intensity* of the laser light can be modulated in the MHz regime using an acousto-optic modulator. On the other hand, a *phase* modulation of the light can be achieved by modulating the diode laser current, which changes the laser frequency and correspondingly the phase.

It may be noted that the modulation frequencies used in our experiment are in the sub-MHz regime, which is within the bandwidth of the unmodulated laser line (1 MHz). This means that the light modulation does not create new frequencies which did not already exist in the unmodulated beam. An important point is that the sidebands have a fixed phase relation, which yields after retro-reflection a standing wave in a reference frame moving with a particular velocity. On the other hand, the frequency components within the homogeneous laser line have no stationary phase relation, and therefore cannot form a stationary standing wave in any reference frame.

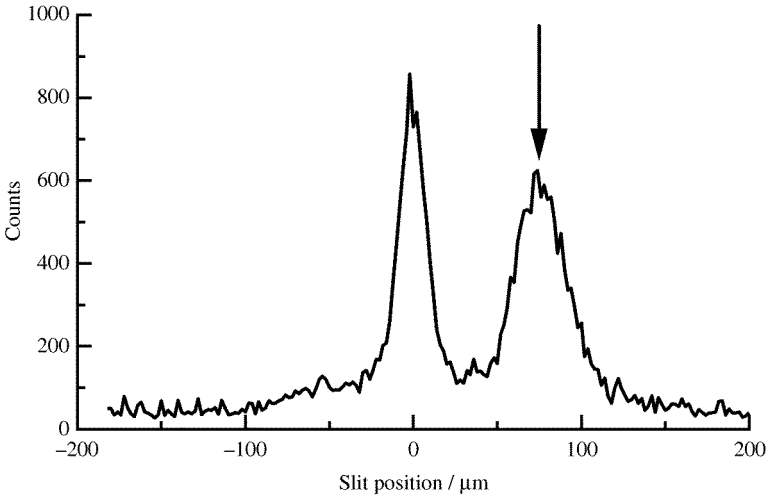

Figure 3. Spatially resolved Bragg diffraction pattern of an argon atomic beam at a stationary standing light wave. A 5 μm slit was scanned in front of the extended channeltron detector in steps of 2 μm. Each data point was elapsed in 1 s. The angle of incidence of the atomic beam into the light wave was exactly the Bragg angle (28 μrad) obtained with our experimental parameters ($v_A = 440$ m s^{-1}, $\lambda_L = 811$ nm). The broader peak (arrow) corresponds to the diffracted beam, whereas the other peak is due to the transmitted part of the de Broglie wave. At other angles of incidence only the transmission peak was observed.

After the interaction region, the atomic beam passes a 137 cm long separation section in order to isolate diffracted and undiffracted beams. The spatial diffraction patterns are resolved by scanning a 5 μm slit in front of the channeltron detector and measuring the beam intensity as a function of the slit position. Figure 3 shows a typical result for the case of static Bragg diffraction. The narrower, higher peak corresponds to the undeflected part of the atomic beam, whereas the broader peak (arrow) is deflected by $2\hbar k$ into the first Bragg diffraction order. As expected, no diffraction into the conjugated order is observed, which is indicated by the absence of a third peak located symmetrically on the other side of the undeflected beam. The angle of the mirror surface with respect to the atomic beam was adjusted for this scan to the Bragg angle of 28 μrad. The width of the transmitted peak (FWHM $\approx$ 18 μm) shows the spatial resolution of our experiment. The width of the diffracted peak (FWHM $\approx$ 36 μm) corresponds to this resolution (18 μm) plus an additional term (also 18 μm), which results from the fact, that the diffracted atoms have a residual velocity distribution of approximately 25% (FWHM) around their mean value of 440 m s^{-1}, due to the velocity selection of our Bragg crystal. On the other hand, the transverse velocity ($2\hbar k_L/m \approx 2.5$ cm s^{-1}) is identical for all diffracted atoms. Thus, the longitudinal velocity distribution transforms into a time-of-flight distribution in the 137 cm separation section, resulting in a spatial broadening of the peak in the detector plane. The value of the additional broadening (19 μm) calculated with our assumed velocity distribution of 25% agrees with the experimental value (18 μm) within the experimental resolution.

For investigating diffraction at travelling light gratings, the detection slit was fixed at the peak of the first diffraction order, as marked by the arrow in figure 3. As already mentioned, the spatial position of the Bragg deflected beam is expected to stay constant, independent of the modulation frequency. Figure 4 shows what happens if the mirror angle is now detuned by a certain amount (approximately 75 μrad) from the stationary Bragg angle, and

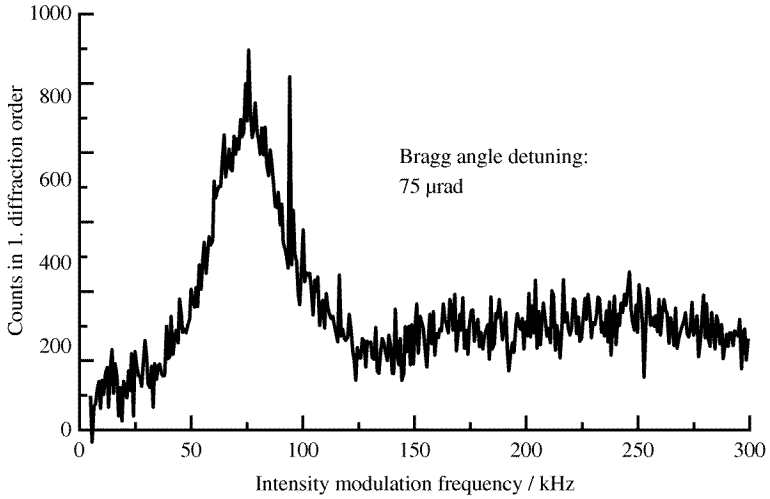

Figure 4. Bragg diffraction efficiency as a function of the light intensity modulation frequency, at an angle detuned by 75 μrad from the stationary Bragg angle. The detection slit position is exactly in the first Bragg diffraction order as indicated in figure 3 (arrow). Without intensity modulation, almost no diffracted signal is observed, due to the Bragg angle detuning. If the light modulation frequency is increased, the diffraction efficiency passes through a maximum at 75 kHz, at which the Bragg angle detuning is compensated by diffraction at a travelling component of the light crystal. The corresponding propagation velocity of the standing wave is 10 cm s^{-1}. By using *phase*- instead of *intensity*-modulated light no diffraction at detuned Bragg angles was observed.

the laser light is now intensity modulated, with a slowly increasing modulation frequency in the range from 5 kHz to 300 kHz in 20 s, with a resolution of 1 kHz. The frequency scans were performed repetitively and integrated for approximately 30 minutes in order to average over laser jitter and atomic beam fluctuations. At low modulation frequencies, a low count rate of the diffracted beam is observed. By increasing the intensity modulation frequency, the intensity of the diffracted beam rises and passes through a maximum at a frequency of 75 kHz, which is expected for a Bragg angle detuning of 70 μrad and an atomic beam velocity of 440 m s^{-1} according to equation (13), and which corresponds to our experimentally adjusted angle (75 ± 6 μrad) within the experimental accuracy. The width of the peak (FWHM $\approx$ 40 kHz $\approx$ 53%) is mainly determined by the velocity distribution (60%) of our atomic beam, and not by the velocity selectivity of our light crystal (25%). This is because during a frequency scan the diffraction condition (equation (13)) is fulfilled successively for all velocity components of the atomic beam. It should be noted that the narrow peak at 96 kHz consists of one single data point which was not reproduced in other experiments and is thus assumed to be noise. The data shows clearly that a detuned Bragg angle results in a suppression of Bragg diffraction, but this detuning can be compensated for by an intensity modulation of the light crystal.

An identical experiment with phase-modulated light has not yet been performed, due to the fact that a continuously scanning phase modulation frequency was not available at this time. Instead, constant frequency sidebands were created by modulating the diode laser frequency according to $E = \exp\{it[\omega_L + \omega_D \sin(\omega_M t)]\}$, where ω_L was the central light frequency, $\omega_D = 2\pi \times 150$ kHz was the maximal frequency deviation and $\omega_M = 2\pi \times 75$ kHz was the modulation rate. Such a frequency modulation is equivalent to a phase modulation

$E = \exp\{i\omega_L t + i\beta \sin(\omega_M t)\}$ with a phase modulation index $\beta = 2$, which is close to the optimal value for first-order sideband production. The sidebands were thus separated by ± 75 kHz from the centre frequency, which is almost the same situation as in the previous experiment, where the intensity modulation frequency at the peak of the diffraction efficiency was also 75 kHz (figure 4) at the detuned Bragg angle. Nevertheless, this time with the frequency-modulated light field, no Bragg diffraction was observed at the same detuned Bragg angle position. A scan of the mirror angle also showed that no diffraction at other angles, with the exception of the 'normal' stationary Bragg angle, occurred.

As explained above, the suppression of diffraction at the travelling waves is due to the fact that the diffraction contributions of the two components, which contribute to each travelling wave, are interfering destructively during the travelling time of the atom through the interaction region. Nevertheless, there might be a small effect due to diffraction at the travelling wave formed by superposition of the two sidebands (case (iii)), which we could not observe to date. Further experiments with improved phase modulation methods are planned to check whether this is due to experimental limits or destructive interference effects of higher-frequency sidebands which are always produced by phase modulation of light waves.

7. Summary

We demonstrated for the first time Bragg diffraction of de Broglie waves at travelling light waves, which results in a change of the Bragg angle. The travelling waves are created in front of a mirror surface by retro-reflecting a modulated light wave. The modulation produces frequency sidebands, resulting in a superposition of slowly travelling intensity gratings with different velocities and directions. Nevertheless, due to the angular selectivity of Bragg scattering, at most one single velocity component can cause diffraction. An interesting feature of travelling waves created by our method is that two contributions with the same velocity diffract simultaneously, and can interfere. We demonstrated that this type of interference is constructive in the case of intensity-modulated light, and destructive in the case of phase-modulated light.

Bragg diffraction at travelling light waves opens a wide field of applications in fundamental research. It is closely related to diffraction-in-time studies. It is particularly interesting to have a coherent, easily controllable frequency shifter for de Broglie waves, an analogue to an acousto-optical modulator for light waves, even with the advantage of producing almost no angular deflection from the static case, as acousto-optical modulators normally do. Other studies, such as diffraction at accelerated light crystals, can be performed in an analogous way, giving more insight into time-dependent de Broglie wave manipulations. By changing the intensity modulation frequency in a controlled manner, even phase modulation of de Broglie waves can be realized. A direct proof of the frequency shift of the deflected wave can be obtained by beating it with the non-shifted centre wave in a Mach–Zehnder interferometer, where time-dependent beating should be observable. This is a goal of ongoing investigations.

Practical applications of this type of Bragg diffraction could arise in atomic lithography. Bragg diffraction provides an atom optical coherent beamsplitter, whose efficiency is continuously tunable between 0 and 100%. The Bragg diffraction at travelling light waves allows this type of diffraction to be achieved without mechanically moving the mirror, merely by adapting the modulation frequency, which could be a great advantage in atom deposition applications.

Acknowledgment

This work was supported by the Austrian Science Foundation (FWF), project number S06504.

References

[1] Martin P J, Oldaker B G, Miklich H and Pritchard D E 1988 *Phys. Rev. Lett.* **60** 512–8
[2] Giltner D M, McGowan R W and Lee S A 1995 *Phys. Rev.* A **52** 3966
[3] Giltner D M, McGowan R W and Lee S A 1995 *Phys. Rev. Lett.* **75** 2638
[4] Gaehler R and Golub R 1984 *Z. Phys.* B **56** 5
[5] Felber J, Mueller G, Gaehler R and Golub R 1990 *Physica* **162B** 191
[6] Felber J 1994 *PhD Thesis* TU-München
[7] Kulda J, Vrana M and Mikula P 1988 *Physica* **151B** 122
[8] Steyerl A 1975 *Nucl. Instrum. Methods* **125** 461
[9] Henkel C, Steane A M, Kaiser R and Dalibard J 1994 *J. Physique II* **4** 1877–96
[10] Steane A, Szriftgiser P, Desbiolles P and Dalibard J 1995 *Phys. Rev. Lett.* **74** 4972
[11] Stenlake B W, Littler I C M, Bachor H-A, Baldwin K G H and Fisk P T H 1994 *Phys. Rev.* A **49** R16
[12] Pritchard D E and Gould P L 1985 *J. Opt. Soc. Am.* B **2** 1799
[13] Reid J and Oka T 1977 *Phys. Rev. Lett.* **38** 67
[14] Arimondo E, Lew H and Oka T 1979 *Phys. Rev. Lett.* **43** 753
[15] Kyrola E and Stenholm S 1977 *Opt. Commun.* **22** 123
[16] Minogin V G and Serimaa O T 1979 *Opt. Commun.* **30** 373
[17] Moore F L, Robinson J C, Bharucha C F, Sundaram B and Raizen M G 1996 *Phys. Rev. Lett.* submitted
[18] Stenholm S 1992 *Proc. Int. School of Phys. (Enrico Fermi, 1991)* ed E Arimondo, W D Phillips and F Strumia p 29–70
[19] Cowley J M 1990 *Diffraction Physics* 2nd edn, 4th print (Amsterdam: North-Holland) ch 8.1, p 162
[20] Salomon C, Dalibard J, Aspect A, Metcalf H and Cohen-Tannoudji C 1987 *Phys. Rev. Lett.* **59** 1659
for an overview see: Balykin V I 1992 *Proc. Int. School of Phys. (Enrico Fermi, 1991)* ed E Arimondo, W D Phillips and F Strumia p 423–66
[21] Batelaan H, Rasel E M, Oberthaler M, Schmiedmayer J and Zeilinger A to be published
[22] Collier R J, Burckhardt C B and Lin L H 1971 *Optical Holography* (New York: Academic)
[23] Kogelnik H 1969 *Bell. Syst. Tech. J.* **48** 2909–47
[24] Kawanaka J, Hagiuda M, Shimizu K, Shimizu F and Takuma H 1993 *Appl. Phys.* B **56** 21–4